

Monte Carlo simulation of a charged fluid separated by a charged wall of finite thickness

Léo Degrève¹ and Marcelo Lozada-Cassou²

¹*Faculdade de Filosofia, Ciências e Letras, Universidade de São Paulo, 14040-901 Ribeirão Preto, São Paulo, Brazil*

²*Departamento de Física, Universidad Autónoma Metropolitana-Iztapalapa,*

Apartado Postal 55-534, 09340 México, Distrito Federal, Mexico

(Received 19 September 1997)

A charged fluid separated by a charged flat wall of finite thickness is studied by means of Monte Carlo computer simulations. Three different approaches of computer simulations are used. It is shown that in simulations of inhomogeneous charged fluids no local electroneutrality condition should be imposed. In agreement with previous studies [M. Lozada-Cassou and J. Yu, Phys. Rev. Lett. **77**, 4019 (1996)] a correlation between the fluids at both sides of the plate is found. Good agreement with theory is obtained.

[S1063-651X(98)09203-4]

PACS number(s): 61.20.Qg, 61.20.Gy

I. INTRODUCTION

When a charged fluid is next to a charged electrode an electrical double layer (EDL) is formed, i.e., the negative and positive charges are arranged such that the electrical field produced by the external field is canceled. At a certain distance away from the electrode the effective electrical field is zero. This distance defines the thickness of the EDL. The structure of this EDL is relevant for some biological [1] and colloidal systems [2–4]. A model for a surface as complex as that of a membrane of a cell or vesicle or a platelike colloidal particle in contact with an ionic fluid is necessarily simple. A widely used model for an ionic fluid next to a charged plate is that in which the electrolyte is assumed to be a fluid of charged hard spheres of charge $e z_i$ and diameter a , in a dielectric continuum of dielectric constant ϵ , where e is the electronic charge and z_i is the valence of an ion of species i . The bulk concentration of the species i is ρ_i and the fluid is assumed to be in equilibrium at a temperature T . This model for an electrolyte is known in the literature as the restricted primitive model (RPM) [4–6]. The plate is considered to be a flat, hard wall with a constant surface charge density. The wall is infinitely thick and is composed of a dielectric material with a dielectric constant chosen to be equal to that of the solvent, for simplicity, such that image forces need not be considered. Liquid theories for inhomogeneous charged fluids have been developed in the past [5,6]. Because real systems are very complex, computer simulations for this model have been made to test these theories, i.e., Monte Carlo (MC) [7–12] and grand canonical Monte Carlo (GCMC) [12,13] simulations. The disagreement of a liquid theory, applied to a simple model, with experimental data could be due to shortcomings of the theory or of the model. Therefore, in the field of the many-body theory for liquids, the use of computer simulations is necessary to progress. The hypernetted-chain (HNC) mean spherical approximation (MSA) theory has been applied to the model described above [5,6]. The agreement of the HNC-MSA results with MC data is good [5,14]. In spite of its simplicity, this model has proved to be successful in reproducing qualitative behaviors of *real* systems [2–4,15].

Recently, the HNC-MSA theory was applied to a RPM

next to a charged wall of *finite* thickness [16]. A correlation between the charged liquids at both sides of the wall was predicted. This effect, if it is real, could be relevant for some biological and complex fluids systems. In this paper we use three methods to simulate an electrolyte solution in contact with a planar wall of finite thickness. Probably because this effect has just been recently detected, all the existing simulations in the literature, to the best of our knowledge, are for walls of infinite thickness.

II. MONTE CARLO METHOD

Reduced concentration profiles (RCPs) were obtained from canonical and grand canonical Monte Carlo simulations conducted on a RPM electrolyte solution in contact with a flat, hard wall of *finite* thickness. The wall has a surface charge density σ_L on its left-hand side and a surface charge density σ_R on its right-hand side. The wall has a width d and is composed of a dielectric material with a dielectric constant chosen to be equal to that of the solvent, for simplicity, such that image forces need not be considered. In the past a direct method (DM) to derive statistical mechanical theories for inhomogeneous fluids has been proposed [17]. This method is based on the equivalence between particles and fields, i.e., the external field in an inhomogeneous fluid can be taken as just another particle in a homogeneous fluid. The DM has proved to be successful in studying fluids in the presence of external fields of different geometries [18]. An obvious application of this method to the field of computer simulations of inhomogeneous fluids is that in which one takes an electrolyte next to a charged plate (i.e., an inhomogeneous liquid) and places the entire system inside a simulation box for a homogeneous fluid, where the plate is one of the particles. This plate can be conveniently located, say, perpendicular to the x axis and at the center of the box in the x direction. The usual Metropolis MC algorithm [19] can now be applied by checking the acceptance of a change in position at either side of the wall.

The simulation box is defined by $[-L_x, L_x]$ and $[0, L_y]$ in the x , y , and z Cartesian axes, respectively. The planar charged plate is perpendicular to the x axis. The dimensions of the simulation box were chosen in order to allow the de-

scription of the system according to the method of Torrie and co-workers [7,8,20], i.e., the distances from the wall surface to the limit of the box on the x axis must be larger than several κ^{-1} Debye-Hückel distances, where

$$\kappa^2 = \frac{4\pi\beta e^2}{\epsilon} \sum_{i=1}^n \rho_i z_i^2 \quad (1)$$

and $\beta = 1/kT$. k is the Boltzmann constant. Torrie and co-workers suggest that a better way to treat the long-range interactions is obtained by using systems that are very large. In this case, Ewald's sums, which introduce spurious effects, are avoided. Therefore, we have used $\kappa(L_x - d/2) \approx 90$ and $\kappa(L_y) \approx 90$.

For our model the total potential energy of an ion is the sum of the hard-sphere contribution and the total electrostatic potential, which is the sum of the interactions with all the other ions and with the surface electrostatic densities on the wall. As a result of all the interactions the effective, exact, interaction potential of an ion of species i with the rest of the system can be found to be [21,22]

$$u_i(x) = -\frac{4\pi e z_i}{\epsilon} \int_x^\infty (y-x) \rho_{el}(y) dy, \quad x \geq 0, \quad (2)$$

where

$$\rho_{el}(y) = \sum_{i=1}^2 e z_i \rho_i g_{pi}(y) \quad (3)$$

is the charge profile produced by a two species electrolyte and $\rho_i g_{pi}(y)$ is the local concentration of ions of species i , at a distance $x = y$ from the center of the plate and perpendicular to the plate. A similar expression applies for $x \leq 0$. However, in Eq. (2) the plate's surface charges do not appear explicitly because the charge density $\rho_{el}(x)$ has its equilibrium value, whose determination is the objective of the simulation. For this reason, the direct interaction potential must be used. Considering that σ_L is located at $x = -d/2$ and σ_R at $x = d/2$, we have

$$u_i(x) = \frac{-4\pi e z_i}{\epsilon} \left[\sigma_L(|x+d/2|) f\left(\frac{|x+d/2|}{L_y}\right) + \sigma_R(|x-d/2|) f\left(\frac{|x-d/2|}{L_y}\right) \right], \quad (4)$$

where $f(z)$ is the "window" function defined by Torrie and co-workers [8,20]. Results for infinite plates in the y and z directions can be obtained by extrapolation of results from systems where the plates present increasing surface area.

We calculated $L_y = 10a$, $20a$, and $30a$ and several values of the wall's charge and thickness and several electrolytes' bulk concentrations. The differences in the RCPs for the three values of L_y are in general undetectable due to the fluctuations. For example, for $d = a$, the differences in the contact values between the $L_y = 20a$ calculations and those for $L_y = 10a$ are less than 6% and those for $L_y = 30a$ are less than 2%, but the differences in the contact values between the $L_y = 10a$ calculations and those for $L_y = 30a$ are less than 4%. After convergence with Eq. (4), Eq. (2) was used in the

simulation for three additional iterations (with 100 000 cycles each) as a test for consistency. The charge induced by the wall to its left- and right-hand sides on the liquid, σ'_L and σ'_R , are obtained from the simulation's "experimental" charge profiles, i.e.,

$$\sigma'_L = -\int_{-\infty}^{-d/2} \rho_{el}(y) dy, \quad \sigma'_R = -\int_{d/2}^{\infty} \rho_{el}(y) dy. \quad (5)$$

The differences in the predicted σ'_R between the $L_y = 20a$ and $10a$ calculations were in general less than 0.09% and those between the $L_y = 20a$ and $30a$ cases were less than 0.07%. Between the $L_y = 10a$ and $30a$ calculations the agreement was less than 0.03%. For σ'_L the disagreement was in general higher, but in general less than 1%. The total electroneutrality condition (TEC) for the plate plus the electrolyte system states that the charge induced in the liquid, by the wall, must cancel that on the wall, that is, $\sigma_L + \sigma_R = \sigma'_L + \sigma'_R$.

We used three methods to simulate the system: *method 1*, GCMC simulations *without* forced total electroneutrality; *method 2*, GCMC simulations with *forced* total electroneutrality; and *method 3*, canonical MC simulations necessarily with forced total electroneutrality. The results of the three methods are essentially indistinguishable, although they can differ in the rate of convergence and in CPU time: Clearly, method 3 is the fastest. The GCMC simulations were conducted alternating canonical and grand canonical Monte Carlo cycles. During the grand canonical Monte Carlo part, attempts for ion creation or destruction were made with equal probabilities for cations and anions in the first method or of neutral ionic pairs in the second case. For example, the grand canonical conditions in the first method are, for the creation of one ion,

$$1 \left/ \left[1 + \frac{N+1}{zV} \exp(\beta \Delta E_c) \right] \right. \geq \chi, \quad (6)$$

and for a destruction

$$1 \left/ \left[1 + \frac{zV}{N} \exp(\beta \Delta E_d) \right] \right. \geq \chi, \quad (7)$$

where z is the absolute activity of the ion, N is the number of particles in the system, V is the total volume of the system, ΔE_c and ΔE_d are the energy changes observed during the corresponding processes, and χ is a random number uniformly distributed on the interval [0,1].

The use of the standard Metropolis Monte Carlo algorithm for our system is justified since, clearly, the system can be divided into two or more subsystems in order to check the acceptance of a change in position that can occur in the same subsystem or between different subsystems, that is, Eqs. (6) and (7) can be approximated for the consecutive processes of destruction of an ion (from a system containing N ions) at one point of the system and its creation at another point of the system (formed now by $N' = N - 1$ ions) by

$$\left\{ 1 / \left[1 + \frac{zV}{N} \exp(\beta \Delta E_d) \right] \right\} \left\{ 1 / \left[1 + \frac{N' + 1}{zV} \right] \right. \\ \left. \times \exp(\beta \Delta E_c) \right\} \approx \exp(-\beta \Delta E_{fi}) \geq \chi. \quad (8)$$

Since

$$\Delta E_{fi} = \Delta E_d + \Delta E_c \\ = \{E(N-1) - E^{\text{old}}(N)\} + \{E^{\text{new}}(N) - E(N-1)\} \\ = E^{\text{new}}(N) - E^{\text{old}}(N), \quad (9)$$

Eq. (8) is the usual Metropolis criterion. The canonical MC simulation is equivalent to a particle destruction followed by a creation, i.e., the energies of two configurations are compared. The periodic boundary conditions and minimum image conventions were used in the y and z directions and hard uncharged walls were located at $-L_x$ and L_x . Due to the fact that $\kappa(L_x - d/2) \approx 90$, no consequence on the diffuse layer structures was detected due to the adsorption or desorption of the electrolytes on these walls. The system, a 2:2 RPM electrolyte next to a charged plate of *finite* thickness, was simulated at $T=298$ K and with $\varepsilon=78.5$. The bulk concentration of the electrolyte (1.09M or 0.051 in units of a^3) was adjusted by means of the ionic, or mean ionic, activities in the first two methods or by means of the constant number of ions in the third method. The first 10 000 simulation cycles were discarded in the first two methods (2000 for the third method) and 100 000 (20 000 for the third method) complete cycles were used to obtain the final data. The reported results are for $L_y=30a$. For this case around 2400 ions were used in the simulation. For $L_y=10a$ and $20a$, around 300 and 1200 particles were used in the simulations, respectively.

III. RESULTS

In all our calculations the fluid is a 2:2, 1.09M (i.e., 0.051 in units of a^3) electrolyte and the ionic diameter was taken to be equal to 4.25 Å. In Fig. 1 the surface charge density on the left-hand side of the wall is $\sigma_L = -0.1419$ C/m² and on the right-hand side $\sigma_R = 0.6741$ C/m². Two thicknesses of the wall are considered: $d=a$ and $500a$. We show the MC positive-ion reduced concentration profile (PIRCP) and the negative-ion reduced concentration profile (NIRCP) induced by the wall in the solution. On the left-hand side of the wall, near the wall, and for $d=a$, the PIRCP is lower than in the bulk solution, whereas the NIRCP is clearly above its bulk value. On the right-hand side of the wall, for $d=a$ the PIRCP is lower than one and the NIRCP is well above one. For a wall thickness of $d=500a$, the PIRCP is well above one on the left-hand side of the wall and lower than one on the right-hand side, whereas the NIRCP is lower than one on the left and higher than one on the right. A calculation for a symmetrically charged wall, with surface charge density equal to -0.1419 C/m², gives a PIRCP and a NIRCP equal to those shown in Fig. 1 for the left-hand side of the wall with $d=500a$. A similar result is observed from a calculation for a symmetrically charged wall, with charge density equal to 0.6741 C/m², i.e., its NIRCP and PIRCP agree with those shown in Fig. 1 for the right-hand side of the d

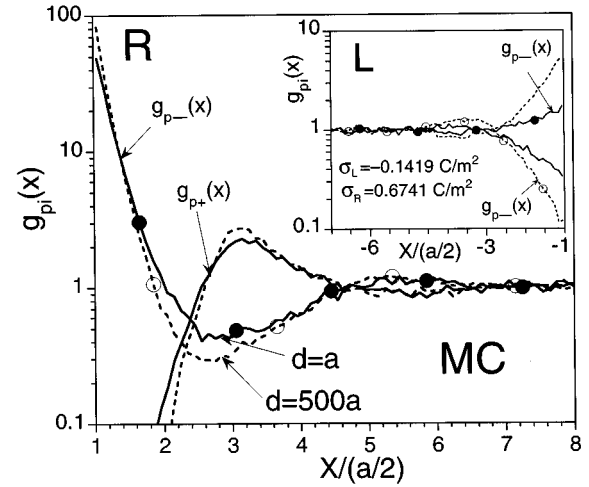


FIG. 1. Monte Carlo RCPs for a 2:2, 1.09M electrolyte, next to a charged wall, as a function of the distance to the wall. The surface charge density on the left-hand side of the wall is $\sigma_L = -0.1419$ C/m² and on the right-hand side $\sigma_R = 0.6741$ C/m². Two thicknesses of the wall are considered: $d=a$ and $500a$. The distance to the wall is expressed in units of the ionic radius. The zero of the x coordinate is located on the left surface of the wall for the left RCPs and on the right surface of the wall for the right RCPs, i.e., the thickness of the wall is not plotted. The solid and broken lines are for the $d=a$ and $500a$ RCPs, respectively. The curves with black and white circles are the NIRCPs for $d=a$ and $500a$, respectively. $T=298$ K, $\varepsilon=78.5$, and $a=4.25$ Å.

$=500a$ wall. For a symmetrically charged plate the NIRCP and PIRCP are independent of the width of the plate. Our results clearly show that there is a correlation between the liquids on both sides of the wall, for thin plates, and that this correlation disappears for very thick plates.

In Fig. 2 the surface charge density on the left-hand side of the wall is $\sigma_L = -0.3$ C/m² and on the right-hand side

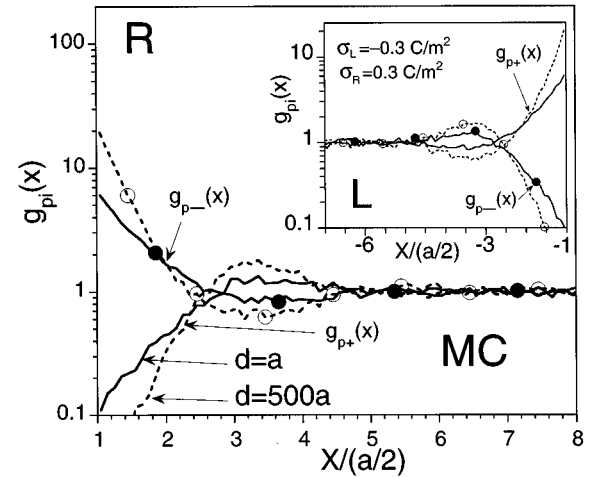


FIG. 2. Monte Carlo RCPs for a 2:2, 1.09M electrolyte, next to a charged wall, as a function of the distance to the wall. The surface charge density on the left-hand side of the wall is $\sigma_L = -0.3$ C/m² and on the right-hand side $\sigma_R = 0.3$ C/m². Two thicknesses of the wall are considered: $d=a$ and $500a$. The meaning of the curves is the same as in Fig. 1. $T=298$ K, $\varepsilon=78.5$, and $a=4.25$ Å.

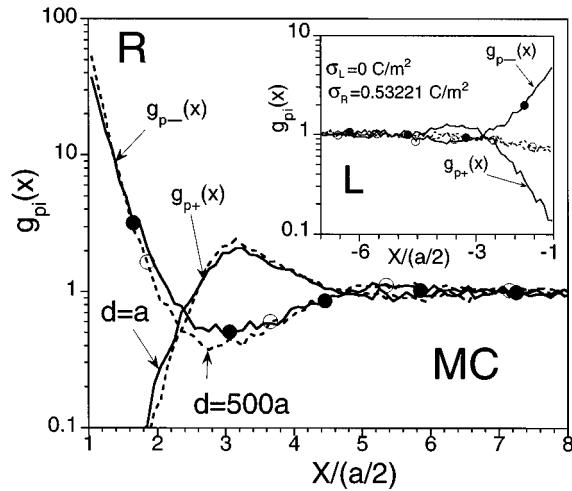


FIG. 3. Monte Carlo RCPs for a 2:2, 1.09M electrolyte, next to a charged wall, as a function of the distance to the wall. The surface charge density on the left-hand side of the wall is $\sigma_L=0 \text{ C/m}^2$ and on the right-hand side $\sigma_R=0.53221 \text{ C/m}^2$. Two thicknesses of the wall are considered: $d=a$ and $500a$. The meaning of the curves is the same as in Fig. 1. $T=298 \text{ K}$, $\epsilon=78.5$, and $a=4.25 \text{ \AA}$.

$\sigma_R=0.3 \text{ C/m}^2$. Two thicknesses of the wall are considered: $d=a$ and $500a$. At the right of the plate, the RCPs have the same qualitative behavior as the corresponding RCPs seen in Fig. 1. Their contact values are considerably lower than those in Fig. 1 due to the lower right surface charge density σ_R . At the left of the plate the $d=500a$ RCPs have the same qualitative behavior as the corresponding RCPs in Fig. 1. The NIRCP and the PIRCP for the $d=a$ case have the opposite qualitative behavior to that in Fig. 1. This shows that in spite of the correlation with the fluid at the other side of the plate, the fluid on the left-hand side of the plate sees a negatively charged plate. Notice, however, that although the net charge of the plate is zero, the fluid “sees” a charged plate. This shows the nonlinear nature of the correlation of the fluids on both sides of the plate.

In Fig. 3 the surface charge density on the left-hand side of the wall is $\sigma_L=0 \text{ C/m}^2$ and on the right-hand side $\sigma_R=0.53221 \text{ C/m}^2$. Two thicknesses of the wall are considered: $d=a$ and $500a$. The qualitative behavior of all the left RCPs and the right, $d=a$, RCPs is similar to that shown in Fig. 2. The left NIRCP and PIRCP, for $d=500a$, become equal and slightly less than one near the plate. Since for $d=500a$ there is no correlation with the liquid on the other side of the plate and the left surface of the plate is uncharged, it is to be expected that the left NIRCP and PIRCP become equal to each other. The drying effect is a consequence of the attractive mean energy of an electrolyte solution.

In Figs. 4–6 we show the HNC-MSA results for the PIRCP and NIRCP induced by the wall in the solution. The electrolyte and plate parameters in Figs. 4–6 are equal to those in Figs. 1–3, respectively. The qualitative behavior of the HNC-MSA concentration profiles is in remarkably good agreement with the MC profiles. The HNC-MSA contact values are consistently higher than those from MC calculations. However, in general, the quantitative agreement between the MC and HNC-MSA concentration profiles is good. In Fig. 6 the left NIRCP and PIRCP, for $d=500a$, reduce to the RCPs

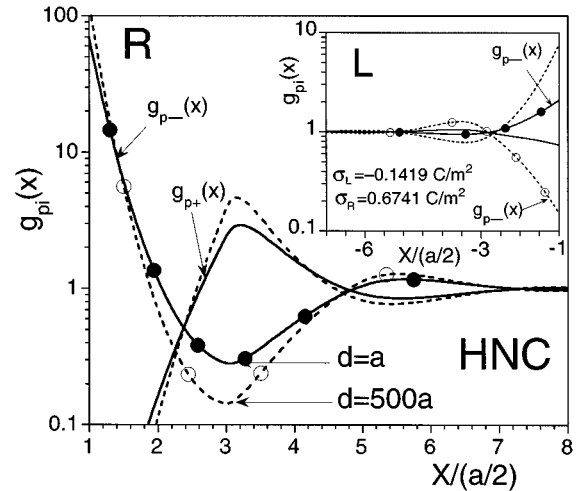


FIG. 4. HNC-MSA reduced concentration profiles for the same parameters as in Fig. 1. The meaning of the curves is the same as in Fig. 1.

for a hard-sphere fluid next to a hard wall, i.e., the left NIRCP and PIRCP become equal and slightly higher than one near the plate. This is probably due to the fact that in the HNC-MSA theory bridge diagrams are lacking.

In Fig. 7 the fluid and the charge of the plate are the same as in Fig. 1. We plot the MC and HNC-MSA results for the charge density induced in the fluid by the wall, as a function of the wall’s thickness. The HNC-MSA results are in very good agreement with our MC data. As d increases, σ'_L decreases and σ'_R increases, such that $\sigma'_L \rightarrow -0.1419 \text{ C/m}^2$ and $\sigma'_R \rightarrow 0.6741 \text{ C/m}^2$ for large values of d . For all situations we find that $\sigma_L + \sigma_R = \sigma'_L + \sigma'_R$. However, we find that in general $\sigma'_L \neq \sigma_L$ and $\sigma'_R \neq \sigma_R$. This implies a violation of some sort of a local electroneutrality condition (LEC).

IV. CONCLUSIONS

Our simulation data shown in Figs. 1–3 and 7 conclusively demonstrate that there is a correlation between liquids

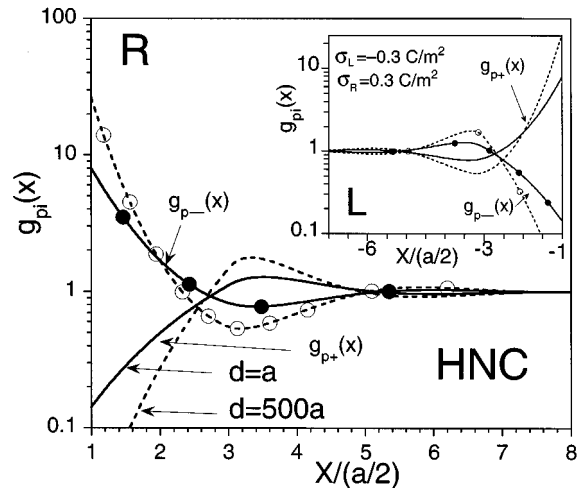


FIG. 5. HNC-MSA reduced concentration profiles for the same parameters as in Fig. 2. The meaning of the curves is the same as in Fig. 1.

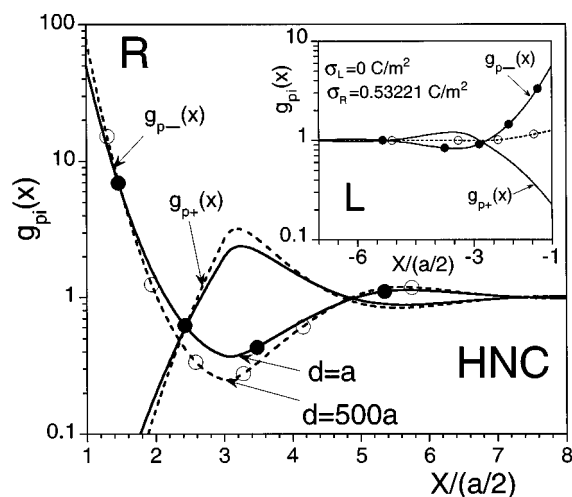


FIG. 6. HNC-MSA reduced concentration profiles for the same parameters as in Fig. 3. The meaning of the curves is the same as in Fig. 1.

on both sides of a wall of finite thickness. The qualitative behavior of our MC data is in complete agreement with that given in Ref. [16]. The fact that σ'_L is in general different from σ_L implies a violation of some kind of LEC [21–23]. However, the TEC $\sigma_L + \sigma_R = \sigma'_L + \sigma'_R$ is indeed satisfied. For a plate of finite thickness the correlation of particles on both sides of the wall produces the violation of the LEC. The agreement of the HNC-MSA results with our simulation data is good. The results of our method 1, where the TEC is not forced, but a constant chemical potential is imposed, show the physically appealing result that electroneutrality is a consequence of the energy equilibrium of the system, not the opposite. Further, we also find that in general the LEC will not be satisfied. Apparently these facts have not been recognized in the literature. Instead there seems to be the general belief that a LEC must be imposed [2–14]. The equivalence between particles and fields, used in the DM, implies that the external field producing the inhomogeneity can be treated as just another particle in the fluid. This method has been successfully applied in the field of integral equations for inhomogeneous fluids [16–18,21–23]. Here we have extended this method to be applied to numerical simulations of inho-

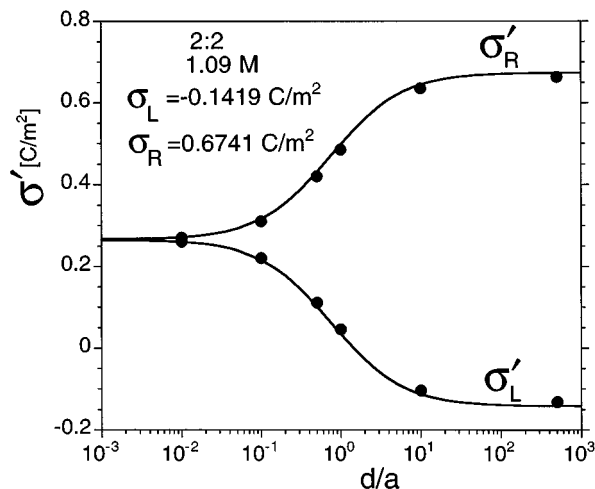


FIG. 7. Charge density induced in the fluid by the wall, as a function of the wall's thickness (expressed in units of the ionic diameter). The fluid and the charge of the plate are the same as in Fig. 1. σ'_L is the charge induced on the left-hand side of the wall, whereas σ'_R is that induced on the right-hand side of the wall. The solid line is the HNC-MSA results and the black dots are the MC data.

mogeneous fluids. This is consistent with the fact that there is no restriction in the partition function related to the homogeneity of the systems. Thus the standard Metropolis MC algorithm can be applied to a fluid separated by a wall by checking the acceptance ratio of a change in position of particles on either side of the wall, as an equivalent method to the GCMC method. Our GCMC and MC simulation results corroborate this fact. Apparently, these ideas have not been applied in the past to simulations of inhomogeneous fluids [6–13]. An open charged system at equilibrium must be electroneutral, as a result of the interaction of all the particles in the system. Hence, clearly, our methods 2 (GCMC simulations with the forced TEC) and 3 (canonical MC simulations with the forced TEC) ought to give the same results as those from method 1 (GCMC simulations without the forced TEC). Our results show the equivalence between the canonical MC and the GCMC methods when applied to confined fluids, when the system is properly defined. However, the MC simulation method is of course much more efficient than the GCMC method.

- [1] See, for example, W. Hoppe, W. Lohmann, H. Markl, and H. Ziegler, *Biophysics* (Springer-Verlag, Berlin, 1983).
- [2] E. J. Verwey and J. Th. G. Overbeek, *Theory of Stability of Lyophobic Colloids* (Elsevier, Amsterdam, 1948).
- [3] W. B. Russel, D. A. Saville, and W. R. Schowalter, *Colloidal Dispersions* (Cambridge University Press, Cambridge, 1989).
- [4] K. S. Schmitz, *Macroions in Solution and Colloidal Suspensions* (VCH, New York, 1993).
- [5] M. Lozada-Cassou, R. Saavedra-Barrera, and D. Henderson, *J. Chem. Phys.* **77**, 5150 (1982).
- [6] S. L. Carnie and G. M. Torrie, in *Advances in Chemical Physics*, edited by I. Prigogine and S. A. Rice (Wiley, New York, 1984).
- [7] G. M. Torrie and J. P. Valleau, *Chem. Phys. Lett.* **65**, 343 (1979).
- [8] G. M. Torrie and J. P. Valleau, *J. Chem. Phys.* **73**, 5807 (1980).
- [9] I. Snook and W. van Meegen, *J. Chem. Phys.* **75**, 4104 (1981).
- [10] G. M. Torrie and J. P. Valleau, *J. Phys. Chem.* **86**, 3251 (1982).
- [11] B. Svensson, B. Jönsson, and C. E. Woodward, *J. Phys. Chem.* **94**, 2105 (1990).

- [12] G. Ciccotti, D. Frenkel, and I. R. McDonald, *Simulation of Liquids and Solids. Molecular Dynamics and Monte Carlo Methods in Statistical Mechanics* (North-Holland, Amsterdam, 1990).
- [13] W. van Meegen and I. Snook, *J. Chem. Phys.* **73**, 4656 (1980).
- [14] M. Lozada-Cassou and D. Henderson, *J. Phys. Chem.* **87**, 2821 (1983).
- [15] J. N. Israelachvili and P. M. McGuiggan, *Science* **241**, 795 (1988).
- [16] M. Lozada-Cassou and J. Yu, *Phys. Rev. Lett.* **77**, 4019 (1996); *Phys. Rev. E* **56**, 2958 (1997).
- [17] M. Lozada-Cassou, *J. Chem. Phys.* **75**, 1412 (1981); **77**, 5258 (1982).
- [18] M. Lozada-Cassou, in *Fundamentals of Inhomogeneous Fluids*, edited by D. J. Henderson (Dekker, New York, 1992), Chap. 8.
- [19] N. Metropolis, A. W. Rosenbluth, M. N. Rosenbluth, A. H. Teller, and E. Teller, *J. Chem. Phys.* **21**, 1087 (1953).
- [20] J. P. Valleau, R. Ivok, and G. M. Torrie, *J. Chem. Phys.* **95**, 520 (1991).
- [21] M. Lozada-Cassou, *J. Chem. Phys.* **80**, 3344 (1984).
- [22] M. Lozada-Cassou and E. Díaz-Herrera, *J. Chem. Phys.* **92**, 1194 (1990).
- [23] M. Lozada-Cassou, W. Olivares, and B. Sulbarán, *Phys. Rev. E* **53**, 522 (1996).